

an equilibrium reflection of the nucleation process seen in kinetics experiments.<sup>24,25</sup> Since nucleation kinetics also produces transient length overshoot, the absence of small polymers in the supernatant may also be partially due to incomplete equilibration. We are presently calculating the equilibrium distributions of polymer sizes and orientations, and the corresponding phase diagrams, for nucleated reversible polymerization. It is anticipated that the behavior will be intermediate between that for unconstrained reversible polymerization, as presented here, and constrained reversible polymerization in which monomer and polymer do not coexist in significant amounts in the same phase, as presented previously.<sup>14,15</sup>

**Acknowledgment.** We thank Irene Mendelson for assistance with computing. This work was supported by U.S. Public Health Service Grants AM21077 and HL07451. J.H. is supported by a Faculty Research Award from the American Cancer Society and NIH Grant RR05381.

## References and Notes

- (1) Onsager, L. *Ann. N.Y. Acad. Sci.* **1949**, *51*, 627-59.
- (2) Flory, P. J. *Proc. R. Soc. London, Ser. A* **1956**, *234*, 73-89.
- (3) DiMarzio, E. A. *J. Chem. Phys.* **1961**, *35*, 658-69.
- (4) Robinson, C. *Trans. Faraday Soc.* **1956**, *52*, 571-92.
- (5) Hermans, J. *J. Colloid Sci.* **1962**, *17*, 638-48.
- (6) Nakajima, A.; Hayashi, T.; Ohmori, M. *Biopolymers* **1968**, *6*, 973-82.
- (7) Wee, E. L.; Miller, W. G. *J. Phys. Chem.* **1971**, *75*, 1446-52.
- (8) Miller, W. G.; Wu, C. C.; Wee, E. L.; Santee, G. L.; Rai, J. H.; Goebel, K. G. *Pure Appl. Chem.* **1974**, *37*, 37-58.
- (9) Miller, W. G.; Rai, J. H.; Wee, E. L. *Liq. Cryst. Ordered Fluids* **1974**, *2*, 243-55.
- (10) Papkov, S. L. *Khim. Volokna* **1973**, *15*, 3.
- (11) Papkov, S. P.; Kalichikhin, V. G.; Kalmykova, V. D. *J. Polym. Sci., Polym. Phys. Ed.* **1974**, *12*, 1753-70.
- (12) Morgan, P. W. *Polym. Prepr., Am. Chem. Soc., Div. Polym. Chem.* **1976**, *17*, 47-52.
- (13) Kwolek, S. L.; Morgan, P. W.; Schaefgen, J. R.; Gulrich, L. W. *Polym. Prepr., Am. Chem. Soc., Div. Polym. Chem.* **1976**, *17*, 53-58.
- (14) Briehl, R. W.; Herzfeld, J. *Proc. Natl. Acad. Sci. U.S.A.* **1979**, *76*, 2740-4.
- (15) Herzfeld, J.; Briehl, R. W. *Macromolecules* **1981**, *14*, 397-404.
- (16) Herzfeld, J.; Briehl, R. W. *Ferroelectrics* **1980**, *30*, 125-32.
- (17) Straley, J. P. *J. Chem. Phys.* **1972**, *57*, 3694-5.
- (18) Minton, A. P. *J. Mol. Biol.* **1974**, *82*, 483-98.
- (19) DiMarzio, E. A.; Gibbs, J. H. *J. Chem. Phys.* **1958**, *28*, 807-13.
- (20) Briehl, R. W.; Ewert, S. *J. Mol. Biol.* **1973**, *80*, 445-58.
- (21) Ross, P. D.; Hofrichter, J.; Eaton, W. A. *J. Mol. Biol.* **1975**, *96*, 239-56.
- (22) Ross, P. D.; Hofrichter, J.; Eaton, W. A. *J. Mol. Biol.* **1977**, *115*, 111-34.
- (23) Magdoff-Fairchild, B.; Poillon, W. N.; Li, T.-I.; Bertles, J. F. *Proc. Natl. Acad. Sci. U.S.A.* **1976**, *73*, 990-4.
- (24) Hofrichter, J.; Ross, P. D.; Eaton, W. A. In "Proceedings of the Symposium on Molecular and Cellular Aspects of Sickle Cell Disease"; Hercules, J. I., Cottam, G. L., Waterman, M. R., Schechter, A. N., Eds; Department of Health Education and Welfare: Washington, D.C., 1976; Publication No. (NIH) 76-1007, pp 185-222.
- (25) Hofrichter, J.; Ross, P. D.; Eaton, W. A. *Proc. Natl. Acad. Sci. U.S.A.* **1974**, *71*, 4864-8.

## Configuration Properties of Comb-Branched Polymers

F. L. McCrackin\* and J. Mazur

Polymer Science and Standards Division, National Bureau of Standards, Washington, D.C. 20234. Received December 15, 1980

**ABSTRACT:** Mean-square radii of gyration were computed for comb-branched polymers simulated by chains on a cubic lattice that incorporated both excluded volume and attractive energies between nonbonded segments of the polymer. The ratios  $g$  of the radius of gyration of comb-branched polymer to that of a linear polymer of the same molecular weight at the  $\Theta$  point were found to be larger than the  $g$  ratios calculated by the unrestricted random walk model of the polymer. The calculated  $g$  ratios were compared with experimental measurements. For the comb-branched polymers, the radii of gyration of the backbones and the expansion factors were also calculated. The radii of gyration of the backbones at the  $\Theta$  conditions were greater than those of linear polymers, in contradiction to the random walk model, which requires that they be equal. The calculated expansion factors were less than those of linear polymers, also in contradiction to perturbation theories based on the random walk model, which predict greater expansion factors for branched polymers than for linear polymers.

## Introduction

A branched polymer molecule in solution is less extended than a linear polymer molecule having the same molecular weight. This fact is expressed by the ratio

$$g = \langle s^2 \rangle_b / \langle s^2 \rangle_l < 1 \quad (1)$$

where  $\langle s^2 \rangle_b$  and  $\langle s^2 \rangle_l$  are the mean-square radii of gyration, which will be called the squared radii, of branched and linear polymer, respectively.

The most common method of determining the degree of branching of a polymer is to measure its  $g$  ratio by light scattering or to infer its value from intrinsic viscosity measurements. From a relationship between the  $g$  ratio and the number of branches per molecule for an assumed type of branching (e.g., star, comb, or random), the number of branches is then determined. This relationship is

evaluated for comb-branched polymer in this paper.

By representing polymers at the  $\Theta$  condition as random flight walks, Stockmayer and Zimm obtained the  $g$  ratios for branched polymers in a closed form.<sup>1</sup> For randomly branched comb polymers, Casassa and Berry<sup>2</sup> obtained

$$g = (1 + f\rho)^{-3} \{ 1 + 2f\rho + (2f + f^2)\rho^2 + (3f^2 - 2f)\rho^3 \} \quad (2)$$

where  $f$  is the number of branches per molecule and  $\rho$  is the ratio of the molecular weight of a branch to that of the backbone. Equation 2 was derived for the case of homogeneous molecular weight of backbone and branches, with a random distribution of branch points on the backbone.

In this paper the  $g$  ratios for comb-branched polymers are computed, based on a model that is physically more realistic than the random walk model. In the present model, the branched polymer is simulated by a self-

avoiding walk on a simple cubic lattice. Many comb-branched walks for a series of values of  $f$  and  $\rho$  were generated by a modified Rosenbluth–Rosenbluth method which is described in detail in ref 3. For each walk, the linear backbone was first generated as a self-avoiding walk. Then  $f$  different positions on the walk were randomly chosen: starting at each of these positions, a branch walk which is of a length equal to  $\rho$  times the length of the backbone was generated. The branches were not allowed to self-intersect or to intersect the backbone or the other branches. For each comb-branched walk thus generated, the following quantities were calculated: (1) the squared radius,  $s^2$ , (2) the number of contacts,  $n$ , i.e., the number of pairs of nonbonded segments separated by a distance equal to one lattice spacing, (3)  $s^4$ , the fourth power of the radius, and (4) the squared radii of the backbone in the branched molecules.

It was assumed that the nonbonded segments separated by one lattice spacing, i.e., forming a contact, interact with an attractive energy equal to  $-\epsilon$ . The total energy for a walk is therefore equal to  $-n\epsilon$  and its Boltzmann factor is  $\exp(n\phi)$ , with

$$\phi = -\epsilon/kT \quad (3)$$

where  $k$  is Boltzmann's constant and  $T$  is the temperature. For given values of  $f$  and  $\rho$ , the mean-square radius is then estimated for selected values of  $\phi$  by averaging the squared radii of the calculated configurations, weighted by their Boltzmann factors. That is

$$\langle s^2 \rangle = \sum_i s_i^2 \exp(n_i \phi) / \sum_i \exp(n_i \phi) \quad (4)$$

where  $i$  is the index of the walk. These calculations were performed for several values of  $\phi$  varying from 0.15 to 0.29 and for values of  $f$ , the number of branches, in the range 5–30. The ratios  $\rho$  of the length of a branch to that of the backbone covered the range from 0 to 3. For each value of  $f$  and  $\rho$ , 30 000 walks were generated in 15 batches of 2000 walks each. The mean-square radii of gyration for the walks in each batch were calculated by eq 4. The average and standard deviation of the mean-square radii of gyration were then calculated from these 15 values. All results with a relative error greater than 4% were rejected. For most calculated quantities the relative error was less than 2%.

The Rosenbluth–Rosenbluth method produces accurate values of the squared radii and other configurational parameters for values of the attractive energy parameter  $\phi$  which are close to its  $\Theta$  point value. For linear chains,<sup>3</sup>  $\phi$  equals 0.275 at the  $\Theta$  point. For this reason, the values of  $\phi$  were restricted to the range 0.15–0.29.

The squared radii and other properties of linear polymers and star-branched polymers have been previously calculated<sup>3,4</sup> by the Monte Carlo method which is employed in this paper. The computational algorithm and the error analysis which is relevant to this work are detailed in these papers.

The  $\Theta$  point of a polymer can be defined in various ways. For linear Monte Carlo chains, it was defined in relation to the squared radius as follows: For a given value of the attractive energy parameter  $\phi$ , the squared radius is given by<sup>3</sup>

$$\langle s^2 \rangle = BN^\gamma \quad (5)$$

for chains with sufficiently large  $N$ , the total number of segments. The parameters  $B$  and  $\gamma$  are functions of  $\phi$ . In a simple cubic lattice,  $\gamma$  is 1 for  $\phi = 0.275$ . This defines the  $\Theta$  point for linear chains. The value of  $\langle s^2 \rangle$  for star-branched molecules on the simple cubic lattice was also

Table I  
Estimate of Parameters  $B$  and  $\gamma$  of Eq 5 for a 10-Branch Comb Molecule and Their Dependence on  $\phi$  and  $\rho$

Values of $\gamma$				
$\phi$	$\rho = 0.1$	$\rho = 0.2$	$\rho = 0.5$	$\rho = 1.0$
0.24	1.076	1.073	1.070	1.076
0.26	1.050	1.044	1.037	1.038
0.275	1.029	1.021	1.001	1.010
0.29	0.959	0.966	0.935	0.948

Values of $B$				
$\phi$	$\rho = 0.1$	$\rho = 0.2$	$\rho = 0.5$	$\rho = 1.0$
0.24	0.135	0.111	0.089	0.0765
0.26	0.147	0.124	0.102	0.0907
0.275	0.156	0.134	0.120	0.103
0.29	0.214	0.172	0.170	0.142

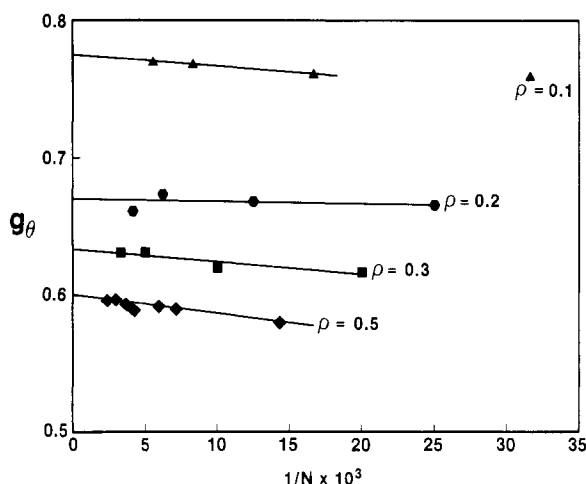


Figure 1. Molecular weight dependence of reduced radii of 5-branch comb polymers at the  $\Theta$  condition.

found to be proportional to  $N$  at the same value of  $\phi = 0.275$ , provided that the number of branches is kept constant.

The squared radii of 10-branch comb-branched chains for  $\rho$  in the range 0.1–1 and  $\phi$  in the range 0.24–0.29 were fit to eq 5. The chains had values of  $N$  from 60 to 1650. Table I shows the values of  $B$  and  $\gamma$  that were obtained. For the lower values of  $\rho$  (0.1 and 0.2) some of the values of  $N$  correspond to very short branches, not sufficiently long to justify the use of the asymptotic equation 5. As Table I indicates,  $\gamma$  is approximately independent of  $\rho$  and reaches the  $\Theta$  value of 1 for  $\phi$  near 0.275, as for linear and star-branched chains. However, the present calculations cannot determine if the  $\Theta$  condition is slightly affected by the amount of branching. Therefore, we will use  $\phi = 0.275$  as the  $\Theta$  point for both linear and branched chains.

#### Calculations of $g$ Ratios for the $\Theta$ Condition

The squared radii for comb-branched chain at the  $\Theta$  point were computed. The subscript  $\Theta$  indicates that the  $g$  ratio is calculated at the value of  $\phi$  corresponding to the  $\Theta$  point. The corresponding  $g_\Theta$  ratios given by eq 1 were computed from the radii. The needed squared radii for long linear chains were calculated from the empirical equation 18 given in ref 4, using the parameters given in Table I of ref 4. This equation is only valid for  $N > 120$ . Therefore, for  $N < 120$ , the values of  $\langle s^2 \rangle_1$  had to be recomputed in conjunction with the present work. In Figure 1,  $g_\Theta$  is shown vs.  $1/N$  for 5-branch comb chains for four different values of  $\rho$ . The variations of  $g_\Theta$  with  $N$  is seen to be small for large  $N$  and the limiting value of  $g$  for infinite  $N$  is readily obtained by extrapolation of the data

Table II  
Experimental, Monte Carlo, and Random Walk Values of  $g_\Theta$  of Comb-Branched Polymers

$f$	$\rho$	$g_\Theta(\text{exptl})$	$g_\Theta(\text{Monte Carlo})$	$g_\Theta(\text{random walk})$	ref
27	0.04	0.576	0.583	0.500	18
26.6	1.32	0.42	0.213	0.13	12
22.6	1.32	0.44	0.231	0.15	12
18.1	1.32	0.46	0.261	0.19	12
28.7	1.80	0.37	0.210	0.12	12
17.8	1.80	0.43	0.260	0.18	12
9.9	1.80	0.56	0.400	0.30	12
9.3	3.67	0.57	0.410	0.30	12
4.6	3.67	0.74	0.610	0.55	12
24	0.035	0.746	0.683	0.56	8
22	0.090	0.612	0.502	0.40	8

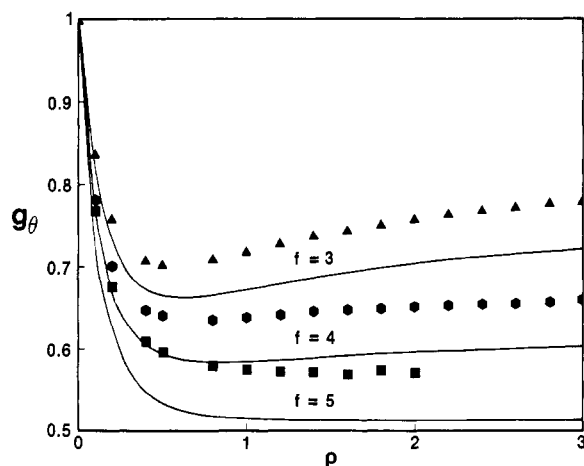


Figure 2. Reduced radii of comb-branched polymers vs.  $\rho$ . Solid lines: random walk model. Calculations for 3-, 4-, and 5-branch polymers. Notice minimums for low values of  $\rho$ .

to  $1/N = 0$ . These limiting values of  $g_\Theta$  are shown in Figures 2 and 3 as functions of  $\rho$ , the ratio of the molecular weight of a branch to that of the backbone. The limiting values of  $g_\Theta$  are shown for 3, 4, and 5 branches in Figure 2 and for 5, 10, and 30 branches in Figure 3. The corresponding random walk values of  $g_\Theta$ , as calculated from eq 2 are shown in those figures by solid lines. The shapes of the curves for the random walk models and for the Monte Carlo computed chains are seen to be similar. Both random walk models and the Monte Carlo computed chains display minima in  $g_\Theta$  vs.  $\rho$  curves for combs with 3 and 4 branches, as shown in Figure 2.

As is evident from Figures 2 and 3, the values of  $g_\Theta$  computed by the Monte Carlo method are greater than the values of  $g_\Theta$  for the random walk model for given values of  $f$  and  $\rho$  and the differences between them increase with increasing number of branches. For 30-branch chains with large  $\rho$ , the values of computed  $g_\Theta$  are almost twice their random walk values.

The values of  $g_\Theta$  for comb-branched chains were fit to the empirical equation

$$g_\Theta = g_\Theta^*(f) + 0.352 \exp(-4.9\rho) + (0.648 - g_\Theta^*) \exp(-27\rho) \quad (6)$$

with  $g_\Theta^*(f) = \lim_{\rho \rightarrow \infty} g_\Theta(f, \rho)$ .

Equation 6 is valid for  $f$  in the range of 5–30. As  $\rho$  approaches infinity,  $g_\Theta$  is seen by eq 6 to approach  $g_\Theta^*(f)$  and the comb-branched chains adopts the shape of a star-branched chain. Therefore,  $g_\Theta^*(f)$  is the value of  $g_\Theta$  for a star-branch chain having  $f$  branches. Equation 6 enables  $g_\Theta$  to be easily calculated for any set of values of  $f$  and  $\rho$  within the indicated range of  $f$ . Values of  $g_\Theta$  based on eq 6 are shown by solid lines on Figure 4 and are compared with the Monte Carlo values.

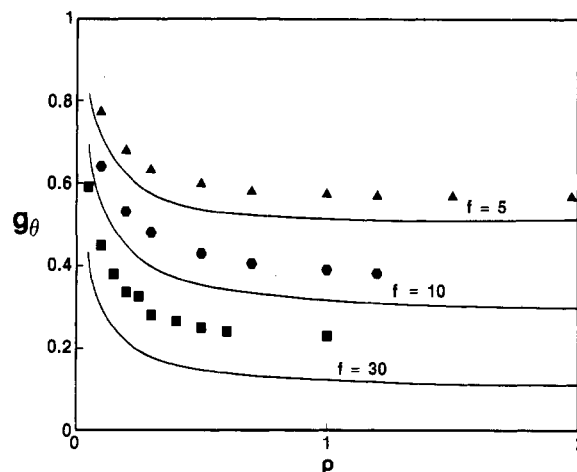


Figure 3. Reduced radii of comb-branched polymers vs.  $\rho$ , the ratio of lengths of branches and backbone. Solid line: random walk model. Calculations for 5-, 10-, and 30-branch polymers in the limit  $n \rightarrow \infty$  for  $\Theta$  conditions.

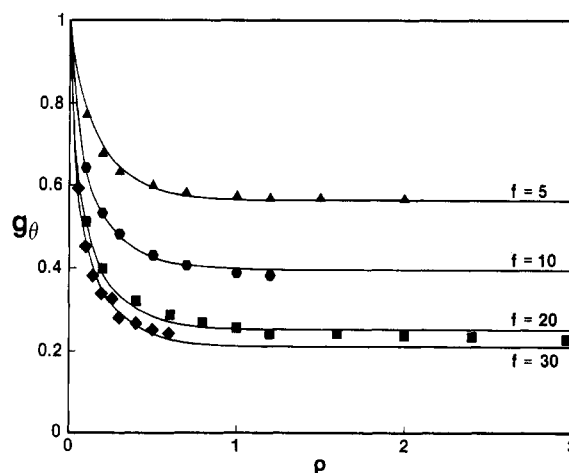


Figure 4. Reduced radii of combs vs.  $\rho$ . Solid lines: empirical fit of data.

The values of  $g_\Theta^*$  obtained by fitting of eq 6 to the  $g_\Theta$  values are shown by the squares in Figure 5. The error in estimating  $g_\Theta^*$  increases with  $f$ . For  $f = 30$ , the standard deviation of  $g_\Theta^*$  is about 0.02. For  $f = 5$ , the estimated value of  $g_\Theta^*$  agrees with the value calculated in ref 4. In ref 4, values of  $g_\Theta^*$  were restricted to  $f \leq 8$ .

The solid line in Figure 5 shows the values of  $g^*$  for the random-walk model calculated from the equation<sup>5</sup>

$$g^* = (3f - 2)/f^2 \quad (7)$$

The random walk values for  $g^*$  are seen to be much smaller than the Monte Carlo values.

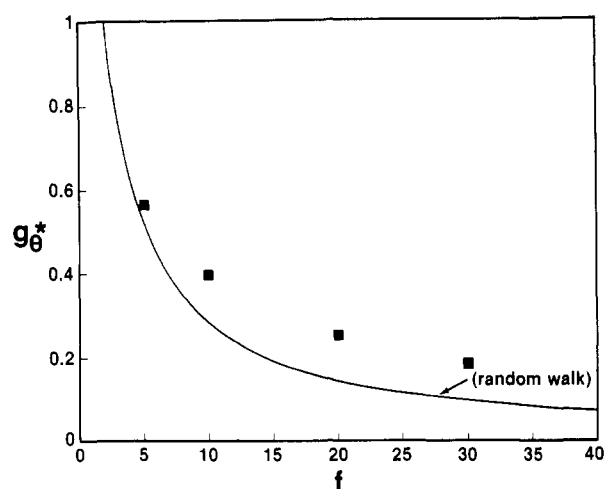


**Figure 5.** Reduced radii of star-branched molecules,  $g_{\theta}^*$ , vs. number of branches.  $g_{\theta}^*$  was obtained by extrapolating  $g_{\theta}^*$  to  $\rho \rightarrow \infty$ . Solid line: random walk stars.  $\theta$  condition.

**Table III**  
Experimental, Monte Carlo, and Random Walk Values of  $g_{\theta}$  for Star-Branched Polymers

$f$	$g_{\theta}(\text{exptl})$	$g_{\theta}(\text{Monte Carlo})$	$g_{\theta}(\text{random walk})$	ref
4	0.65	0.67	0.625	17
4	0.63	0.67	0.625	8
4	0.64	0.67	0.625	9
6	0.42	0.52	0.444	9
6	0.46	0.52	0.444	17
8.7	0.31	0.43	0.318	10
10.7	0.27	0.38	0.263	10
12.3	0.26	0.35	0.231	10
15.3	0.23	0.29	0.187	10
8	0.41	0.44	0.344	6
12	0.33	0.35	0.236	6

Experimental values for  $g_{\theta}$  for comb- and star-branched polymers collected from the literature are presented in Tables II and III. For each experimental value, the corresponding value for the random walk model was computed by eq 2 for comb-branched polymers or by eq 7 for star-branched polymers. The corresponding values of  $g_{\theta}$  for the Monte Carlo model were calculated by eq 6 or were taken from Figure 2. For star-branched polymers, the values of  $g_{\theta}$  were taken from Figure 5 or from ref 4. The experimentally determined values of  $f$  and  $\rho$  were employed throughout.

In Figure 6, the experimental values of  $g_{\theta}$  for comb-branched polymers are plotted vs. the  $g_{\theta}$  values obtained for the Monte Carlo model, and in Figure 7, they are plotted vs. the  $g_{\theta}$  values obtained for the random walk model. On both figures, the experimental values for star-branched polymers are shown by triangles and for comb-branched polymers, by squares. The lines are drawn with a unit slope so that the deviations between experimental and calculated values are shown by the distances of the displayed points from the lines. Because of the large scatter of the experimental data, it is difficult to ascertain whether the Monte Carlo model or the random walk model agrees better with experimental data. As shown in Figures 6 and 7, the experimental  $g$  values for the star-branched chains agree somewhat better with those calculated by the random walk model, while the values for the comb-branched chains appear to agree better with those calculated by the Monte Carlo method.

The calculations in this paper were restricted to the simple cubic lattice. However, previous calculations<sup>4</sup> of star-branched polymers were performed for both simple

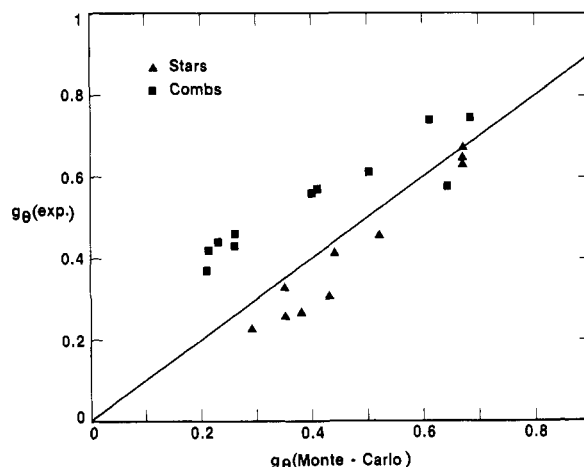


**Figure 6.** Experimental values of  $g$  at the  $\theta$  point vs. the  $g_{\theta}$  values calculated with the Monte Carlo model. The computed  $g_{\theta}$  values are evaluated by using the experimentally determined values of  $f$  and  $\rho$ .

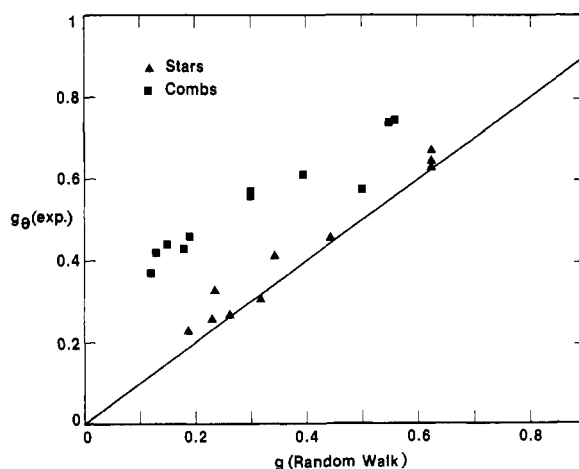


**Figure 7.** Experimental values of  $g$  at the  $\theta$  point vs. the  $g$  values calculated with the random walk model (eq 2).

and face-centered cubic lattices and the reduced radii,  $g_{\theta}^*$ , were the same for both lattices. Therefore, the reduced radii  $g_{\theta}$  computed in this paper are also expected to be independent of the lattice used.

### Expansion Factor

The expansion factor of a polymer is defined as the ratio of the squared radii of the polymer at some value of  $\phi$  and of the same polymer at its  $\theta$  point; that is

$$\alpha^2 = \langle s^2 \rangle_{\phi} / \langle s^2 \rangle_{\theta} \quad (8)$$

For comb-branched chains,  $\alpha^2$  is a function of  $N$ ,  $f$ , and  $\rho$ . In order to present our results in a compact form, independent of molecular weight,  $\alpha^2$  is presented in its reduced form by dividing it by the expansion factor calculated for linear chains. The reduced expansion factors  $\alpha_{\text{comb}}^2 / \alpha_{\text{linear}}^2$  were found to approach limiting values for large  $N$ .

In Figure 8, the extrapolated reduced expansion ratios are shown vs.  $\rho$  for several values of  $\phi$  for the 10-branch combs. In Figure 9, similar results are shown for the 20-branch combs. Figures 8 and 9 demonstrate that the reduced expansion factors are always less than 1. In other words, the power of a good solvent (i.e., having a low value of  $\phi$ ) to expand the molecular dimensions of a polymer over that of a  $\theta$  solvent is diminished by branching. In extreme cases of combs with many long branches (large  $f$  and  $\rho$ ),  $\alpha_{\text{comb}}^2$  tends to approach a value of 1, independent of  $\phi$ .

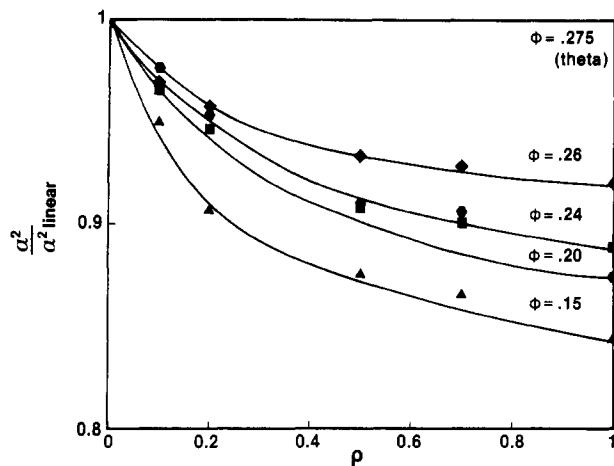


Figure 8. Ratio of expansion factors of comb-branched and linear polymers for 10-branch combs.

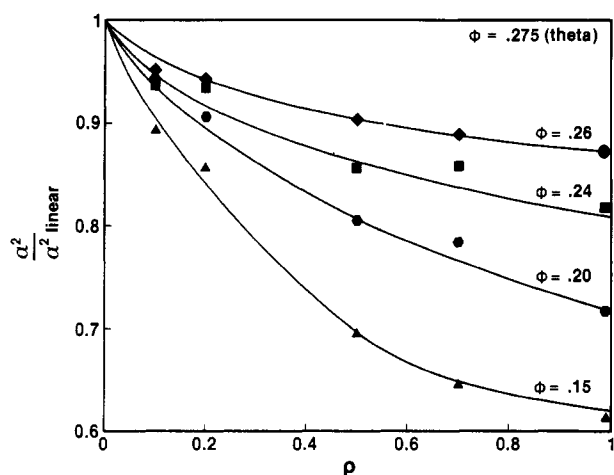


Figure 9. Ratio of expansion factors of comb-branched and linear polymers for 20-branch combs.

It is of interest to notice that the analytical theories<sup>13,14</sup> from which  $\alpha^2$  is evaluated lead to  $\alpha_{\text{comb}}^2/\alpha_{\text{linear}}^2 > 1$ , with this ratio increasing with increasing  $f$  and  $\rho$ . The reason for this discrepancy can be explained along these lines: The analytical model represents the polymer at its  $\Theta$  point by a random walk. The good-solvent effect, which brings about a net repulsion between polymer segments, is subsequently introduced as perturbations to the random walk. These perturbations increase with increased branching, so the expansion factor also increases. The main discrepancy between the analytical and the Monte Carlo calculated results lies in the treatment of the polymer at the  $\Theta$  point. We believe that the random walk is not an adequate model of a polymer at its  $\Theta$  condition on which to base its expansion properties in good solvents.

### Reduced Moments

The calculated fourth reduced moments,  $\langle s_N^4 \rangle / \langle s_N^2 \rangle^2$ , are used to estimate the sharpness of the distribution of the radii of the branched molecules. The closer the fourth reduced moment is to 1, the sharper is the distribution. Calculations of this quantity show that it approaches its limiting value of an infinitely long chain very rapidly. In Figure 10 the extrapolated fourth reduced moments

$$\langle s^4 \rangle / \langle s^2 \rangle^2 \equiv \lim_{N \rightarrow \infty} \langle s_N^4 \rangle / \langle s_N^2 \rangle^2 \quad (9)$$

are plotted vs.  $\rho$  for  $f = 5, 10$ , and  $20$ . The data shown in Figure 10 are for the molecule at its  $\Theta$  condition.

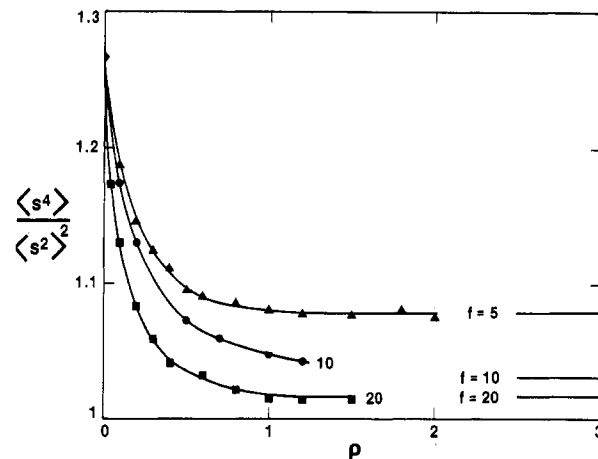


Figure 10. Fourth reduced moments (eq 9) extrapolated to infinite chain length vs.  $\rho$ .

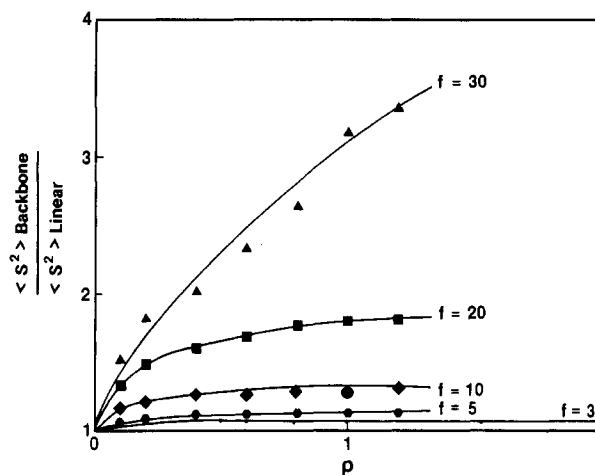


Figure 11. Reduced radii of backbone in comb-branched polymers at the  $\Theta$  condition.

When  $\rho$  is zero, the comb-branched molecule has the shape of a linear molecule. The value of the reduced moment<sup>3</sup> of a linear molecule is therefore shown in Figure 10 for  $\rho = 0$ . When  $\rho$  approaches infinity, the comb-branched molecule approaches the shape of a star-branched molecule. The reduced moments of star-branched polymers having 5, 10, and 20 branches are shown in Figure 10 by horizontal lines. These moments were obtained by extrapolating the data from ref 4 using the fact that for star-branched molecules,  $\lim_{f \rightarrow \infty} \langle s^4 \rangle / \langle s^2 \rangle^2 = 1$ . The reduced moments of comb-branched molecules for a given number of branches,  $f$ , are seen to be smaller than those of linear molecules and greater than those of star molecules. We conclude that the distribution of the radii of comb-branched molecules is sharper than it is for linear molecules but is less sharp than for star-branched molecules.

Solc<sup>15</sup> investigated the reduced moments for comb- and star-branched molecules, using a random walk model. His results are in qualitative agreement with ours.

### Reduced Squared Radii of Backbones

The squared radii for only those segments in the comb-branched chains which constitute their backbones were computed. These squared radii were then divided by the squared radii of a linear chain having the same molecular weight as the comb backbone and the ratios were extrapolated to infinite chain length. These ratios, which are defined as the reduced squared radii of the backbones,

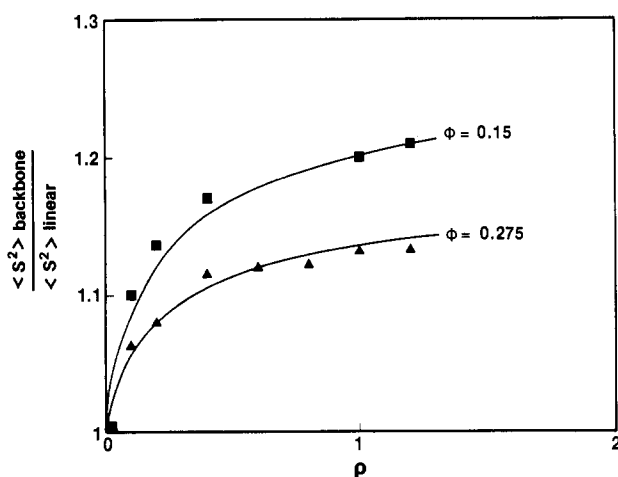


Figure 12. Comparison of reduced radii of backbone in good and in  $\Theta$  solvents for 5-branch comb polymers.

are plotted in Figure 11 vs.  $\rho$  for several values of  $f$ . The data presented in Figure 11 are for chains in their  $\Theta$  conditions. The reduced radii are seen to be greater than 1, so that, even in a  $\Theta$  solvent, the backbone of a comb-branched molecule is more extended than is a linear chain having the same molecular weight. Also, the reduced radii of the backbone are seen to increase with increasing  $\rho$  and  $f$ . It should be remembered that for the random walk model of the polymer at the  $\Theta$  condition, the radius of the backbone is the same as that of a linear molecule of the same molecular weight, independent of the number or length of the branches. Therefore, a measurement of the squared radius of the backbone of a comb-branched polymer at its  $\Theta$  condition would provide a sensitive comparison of the Monte Carlo and random walk models. Such a measurement is planned by Han<sup>16</sup> on a 28-branch comb polystyrene polymer. The branches of the polymer are deuterated while the backbone is protonated. Han plans to measure the small-angle neutron scattering of the polymer in a  $\Theta$  solvent for which the deuterated branches will not scatter the neutrons so that the squared radius of the backbone can be obtained.

In Figure 12, the reduced radii of the backbone of a polymer in a good solvent ( $\phi = 0.15$ ) and in a  $\Theta$  solvent ( $\phi = 0.275$ ) are compared for 5-branch comb polymers. The reduced radius of the backbone is greater in a good solvent than in a  $\Theta$  solvent. This means that the polymer-solvent interactions tend to further expand the backbone in branched as compared to linear polymers.

## Conclusions

The  $g_\Theta$  ratio at the  $\Theta$  point has been computed for comb-branched polymers by a Monte Carlo method. The  $g_\Theta$  ratio was found to be only slightly dependent on  $N$ , the number of segments in the molecule, so the values were readily extrapolated to infinite  $N$ . The extrapolated  $g_\Theta$  ratios increased with the number of branches. Those were larger than the  $g_\Theta$  ratios calculated by the random walk model of the polymer; for 30-branch comb polymers, the Monte Carlo values were almost twice the random walk values.

Values of  $g_\Theta$  computed by both models were compared with experimental values collected from the literature. The experimental values of  $g_\Theta$  agreed equally well with the values computed by the two models.

The expansion factors of the comb-branched polymers were also calculated and found to be less than those of corresponding linear polymers. This contradicts the first-order perturbation calculations superimposed on the

random walk model, which predict that the expansion factors of branched polymers are greater than those of corresponding linear polymers.

The reduced squared radii of only the segments in the backbone of the polymer were also calculated. Values greater than 1 which increase with increasing number of branches were always obtained, even at the  $\Theta$  condition. On the other hand, the random walk model predicts that the squared radius of the backbone of a comb-branched polymer is the same as that of a linear polymer so the reduced radius of the backbone would always be equal to 1. Planned measurements of the reduced radius of the backbone of a comb-branched polymer will therefore serve as a sensitive test of the relative merits of the random walk and the Monte Carlo models of a polymer.

A Monte Carlo model of a polymer at its  $\Theta$  point that includes the excluded volume and the self-interacting properties of a real polymer has been applied to comb-branched polymers. This model may be experimentally compared with the random walk model of the polymer in three ways:

First, the  $g$  ratios calculated for both models may be compared with experimental values. As is seen from the data in Figures 6 and 7, the Monte Carlo and random walk models are shown to give equally good agreement with the experimental  $g$  ratios. However, more accurate experimental  $g$  ratios, especially for star or comb branches, would make the comparison more definite.

Second, experimental measurements of expansion factors would provide a definite comparison between these models because the Monte Carlo model predicts that the expansion factors of branched polymers are smaller than those of linear polymers. However, the opposite result is obtained by theories that represent the polymer at its  $\Theta$  point by the random walk model and introduce the excluded volume effects as a first-order perturbation.

Third, experimental measurements of the radius of the backbone of a branched polymer at its  $\Theta$  point would provide a definite comparison because the Monte Carlo model predicts a larger radius than that of a linear polymer having the same molecular weight, while the random walk model predicts equal radii.

## References and Notes

- (1) Stockmayer, W. H.; Zimm, G. H. *J. Chem. Phys.* **1949**, *17*, 301.
- (2) Casassa, E. F.; Berry, G. C. *J. Polym. Sci., Part A-2* **1966**, *4*, 891.
- (3) McCrackin, F. L.; Mazur, J.; Guttman, C. M. *Macromolecules* **1973**, *6*, 859. Mazur, J.; McCrackin, F. L. *J. Chem. Phys.* **1968**, *49*, 648.
- (4) Mazur, J.; McCrackin, F. L. *Macromolecules* **1977**, *10*, 326.
- (5) Stockmayer, W. H.; Zimm, B. H. *J. Chem. Phys.* **1949**, *17*, 301.
- (6) Bauer, B. J.; Hadjichristidis, N.; Fetters, L. J. *Polym. Prepr., Am. Chem. Soc., Div. Polym. Chem.* **1979**, *20* (2), 126.
- (7) Roovers, J. J. *Am. Chem. Soc.* **1980**, *102*, 2410.
- (8) Berry, G. C. *J. Polym. Sci., Part A-2* **1971**, *9*, 687.
- (9) Roovers, J. E. L.; Bywater, S. *Macromolecules* **1977**, *5*, 384. *Ibid.* **1974**, *7*, 443.
- (10) Meunier, J. C.; van Leemput, R. *Makromol. Chem.* **1971**, *147*, 191.
- (11) Zillox, J. G. *Makromol. Chem.* **1972**, *156*, 121.
- (12) Noda, I.; Horikawa, T.; Kato, T.; Fujimoto, T.; Nagasawa, M. *Macromolecules* **1970**, *3*, 795.
- (13) Casassa, E. F.; Solensky, P. A. *Polym. Prepr., Am. Chem. Soc., Div. Polym. Chem.* **1979**, *20* (2), 171.
- (14) Berry, G. C.; Trofino, T. A. *J. Chem. Phys.* **1964**, *40*, 615.
- (15) Solc, K. *Macromolecules* **1973**, *6*, 378.
- (16) Han, C., private communication.
- (17) Hadjichristidis, N.; Roovers, J. E. L. *J. Polym. Sci., Polym. Phys. Ed.* **1974**, *12*, 2521.
- (18) Roovers, J. E. L., private communication. Roovers measured the radius of gyration of a comb-branched polystyrene in cyclohexane at 35 °C, which is the  $\Theta$  temperature for linear polystyrene. The measured squared radii of the comb-branched polystyrene and of its backbone were 260 and 214

nm<sup>2</sup>, respectively. Also the molecular weights of the comb backbone and single branch were  $5.8 \times 10^5$  and  $1.13 \times 10^4$ , respectively. From these data, we estimated that  $f = 27$  and  $\rho = 0.04$ . Since at 35 °C, the squared radius of linear polystyrene is proportional to the molecular weight, the expected

squared radius of a linear polymer having the same molecular weight as in comb-branched polymer is  $214 \times 5.80/2.75 = 451$  nm<sup>2</sup>. Hence, the  $g$  factor is evaluated as  $214/451 = 0.576$ , in good agreement with the value of 0.587, obtained from eq 6 with the  $g_0^*$  from Figure 5.

## Triple Helix of *Schizophyllum commune* Polysaccharide in Dilute Solution. 4. Light Scattering and Viscosity in Dilute Aqueous Sodium Hydroxide

Y. Kashiwagi, T. Norisuye,\* and H. Fujita

Department of Macromolecular Science, Osaka University, Toyonaka, Osaka 560, Japan.  
Received April 23, 1981

**ABSTRACT:** In previous work, it was deduced from sedimentation equilibrium and hydrodynamic measurements that an extracellular  $\beta$ -1,3-D-glucan schizophyllan is dissolved in water as a trimer assuming a triple-helical structure. The study reported in this paper was undertaken to estimate the pitch and stiffness of this helix from radius of gyration data obtained by a light scattering experiment. In the actual measurement, 0.01 N aqueous NaOH instead of pure water was used as the solvent because it was found that the molecular weights expected for the trimer were obtained only when a small amount of NaOH was added but that this operation did not destroy the helical structure of the trimer. The data for  $\langle S^2 \rangle^{1/2}$  (the radius of gyration) as a function of molecular weight agreed with the prediction that the triple helix should behave like a semiflexible rod. The corresponding data for  $[\eta]$  (the intrinsic viscosity) in 0.01 N NaOH also exhibited features characteristic of a semiflexible rod. These data were analyzed in terms of the known theories for unperturbed wormlike chains, with the result that the pitch per glucose residue and the persistence length of the schizophyllan triple helix are  $0.30 \pm 0.01$  and  $180 \pm 30$  nm, respectively. These values are in agreement with those derived in previous work from viscosity and sedimentation velocity in pure water.

Schizophyllan is an extracellular polysaccharide produced by the fungus *schizophyllum commune*; it consists of linearly linked  $\beta$ -1,3-D-glucose residues with one  $\beta$ -1,6-D-glucose side chain for every three main chain residues.<sup>1,2</sup> As was found in part 1<sup>3</sup> from viscosity and sedimentation equilibrium measurements, this polysaccharide shows very characteristic solubility behavior. Thus it disperses in water as a rodlike trimer with a triple-helical structure, while it disperses in dimethyl sulfoxide (Me<sub>2</sub>SO) as a single randomly coiled chain. In part 3,<sup>4</sup> the pitch, diameter, and stiffness (expressed in terms of the persistence length) of the triple helix were estimated from viscosity and sedimentation velocity data, using appropriate hydrodynamic theories for rigid rods<sup>5,6</sup> and wormlike cylinders.<sup>5,7</sup> Here we report a light scattering study undertaken to evaluate the pitch and stiffness of the schizophyllan triple helix from radius of gyration data as a function of molecular weight. Actually, the experiment was done with water containing 0.01 N sodium hydroxide, rather than pure water, as the solvent for the reason mentioned in the Experimental Section. We also obtained viscosity data in this solvent and used them to estimate the pitch, diameter, and stiffness of the triple helix.

### Experimental Section

**Samples.** Three schizophyllan samples, designated below as K ( $[\eta] = 7 \times 10^2$  cm<sup>3</sup> g<sup>-1</sup> in water at 25 °C), G ( $[\eta] = 4.7 \times 10^2$  cm<sup>3</sup> g<sup>-1</sup>), and H ( $[\eta] = 2.1 \times 10^2$  cm<sup>3</sup> g<sup>-1</sup>), were supplied by Taito Co. They were prepared by sonication of a native schizophyllan and purified by the method described in part 1.<sup>3</sup> By fractional precipitation and extraction with water as a solvent and ethanol as a precipitant, six fractions were separated from sample K, ten fractions from sample G, and eight fractions from sample H. An appropriate middle fraction of each sample was further divided into several parts, and five fractions, designated below as K-4, G-6, G-8, H-3, and H-5, were chosen for the present study. They were reprecipitated from aqueous solutions into acetone and

freeze-dried from aqueous solutions.

Six more samples were used; four of them were a native sample N-1 and sonicated samples S-65-2, S-45-4, and S-164-3, all used in our previous studies<sup>3,4</sup> of this series, and the rest were samples S-100-2 and E-4b chosen from our stock.

Each of these eleven samples was dried overnight in vacuo at room temperature before use.

**Preliminary Experiments.** When we commenced the present light scattering study with pure water solutions, we anticipated that the measurement would give weight-average molecular weights,  $M_w$ , consistent with the values calculated from intrinsic viscosities,  $[\eta]$ , of the same solutions, using the  $[\eta]$  vs.  $M_w$  relation established in part 3.<sup>4</sup> However, the actual values of  $M_w$  were 10–50% higher than the expected ones, and the discrepancy was greater for higher  $M_w$ . We suspected that this was due primarily to our insufficient optical clarification of the solutions and tried more intensive purification by repeating filtration and centrifugation. However, no substantial change occurred in the measured  $M_w$ .

At this stage we abandoned the use of pure water solutions and turned to testing the idea that the major source of the anomaly was the presence of microgels impossible to remove by ordinary means; if so, the problem should be eliminated or minimized by addition of a solubility-enhancing reagent which allows dissociation of those gels. The point is that such a reagent should not be strong enough to break the triple-helical structure of schizophyllan trimers or even to degrade the polymer. We tried to check this idea with potassium chloride and Me<sub>2</sub>SO, but the results were discouraging. Eventually, we tried 0.01 N sodium hydroxide (NaOH) and found  $M_w$  approaching the values expected for trimers. This was encouraging, but we wondered if the stiffness of the helical structure of the trimer was impaired by the alkali. To examine this point we measured  $[\eta]$  of several samples in aqueous NaOH of different concentrations. The experimental results delineated in Figure 1 suggest that the triple helix which schizophyllan would assume in pure water is maintained in aqueous NaOH if the alkali concentration does not exceed 0.02 N. From these observed facts we chose 0.01 N NaOH as the solvent for the present light scattering characterization of the schizophyllan triple helix.